ELSEVIER

Computational Materials Science 9 (1997) 158–167

COMPUTATIONAL MATERIALS SCIENCE

Numerical simulation of deformation induced anisotropy of polycrystals

A. Bertram [a,*], Th. Böhlke [a], M. Kraska [b]

[a] Institut für Mechanik, Otto von Guericke Universität Magdeburg, Postfach 4120, 39016 Magdeburg, Germany
[b] Institut für Mechanik, Sekr. C8, Technische Universität Berlin, Str. d. 17. Juni 135, 10623 Berlin, Germany

Abstract

Aspects of the homogenization problem for polycrystalline materials using finite element based representative volume elements (RVE) are discussed. Special attention is paid to the boundary conditions and the representation of initially isotropic states with limited numbers of grains. The RVE is used for simulations of shear tests with aluminium specimens as reported by Williams [O.W. Williams, Shear textures in copper, brass, aluminium, iron and zirconium, Trans. Met. Soc. AIME 224 (1962) 129–139.]. On the grain level, slip system theory, combining anisotropic elasticity with a viscoplastic flow rule, is used. The resulting texture is represented in the Rodrigues space and by pole figures. Initial and subsequent yield surfaces are investigated using different yield criteria. © 1997 Elsevier Science B.V.

1991 MSC: 73B40; 73E05; 73G20
Keywords: Texture development; Finite plasticity

1. Introduction

The phenomenological theory of material behaviour in the context of continuum mechanics is very successful when applied to many engineering problems. Generally, it is sufficient to derive macroscopic descriptions for particular materials and identify the corresponding parameters by experimental data. However, as soon as large inelastic deformations are involved, things get more complicated. Such deformations may occur during metal forming processes and are accompanied by a considerable change in the macroscopic material behaviour due to microstructural changes. The need for optimal mechanical processing and product functionality provides strong motivation for research in the field of process simulation. It is difficult to model adequately the complex deformation process and the observed material response by means of the traditional macroscopic approach.

A very successful alternative is to derive the macroscopic behaviour of polycrystalline metals from its constituents, considered as single crystals. Within certain limitations, crystal plasticity can be described using the concept of slip systems. This concept is capable of accounting for lattice rotations at large strains and uses a one-dimensional material law. After accepting the fact that many physical effects such as diffusion and recrystallization are beyond the current capabilities of crystal plasticity, the problem consists in modelling the evolution of the macroscopic material behaviour as a result of microstructural changes. This represents the so-called *homogenization* problem.

For large deformation plasticity, there are mainly four homogenization concepts:

Taylor theory: The local strain field is assumed to be constant in space and, thus, equal to the global strain. The global stress is obtained by averaging over all grains. Compatibility of the aggregate is identically preserved, but in general intergranular equilibrium is violated.

Sachs theory: This is the counterpart to Taylor's theory. The local stress field is assumed to be constant in space and equal to the global stress tensor. As a consequence each grain deforms uniformly. Global strain results from averaging over the grains. Thus, the equilibrium condition is identically fulfilled, but compatibility between grains is generally violated.

Self consistent schemes: Each grain is considered to be separately embedded in a homogeneous equivalent medium (HEM). The stress and strain fields far from the inclusion are homogeneous and their values are taken as the global ones. The deformation and stress of each grain are obtained by solution of a separate boundary value problem. The constants of the phenomenological constitutive law for the HEM are iterated until the HEM behaves like the average of the grains. Thus, an inverse problem has to be solved. Compatibility and equilibrium condition are fulfilled only between single grains and the surrounding HEM.

Representative volume elements (RVE): At some macroscopic material point, a small volume is cut out of the body. For this volume, the boundary value problem is solved in order to obtain the overall material response of the volume. The RVE has to be large enough to be a really representative one. The complexity a given simulation can describe is in principle restricted only by local model and the available computational facilities.

The last approach is principally capable of accounting for equilibrium and compatibility anywhere in the microscopically heterogeneous structure. This method is open to direct implementation of, for example, grain shape and grain boundary effects.

* Corresponding author.

PII S0927-0256(97)00071-2

2. Representative volume element

2.1. Homogenization procedure

Our aim is to obtain a relation at some material point X of the body $\mathscr{B}$ between the local stress field $T(X)$ and the global stress $\bar{T}$, as well as between the local deformation field $F(X)$ and the global deformation $\bar{F}$. The basic idea is to split the displacement field $u(X)$ into two parts, one corresponding to a homogeneous global deformation, and the other to a local fluctuating part $w(X)$

$$u(X) = (\bar{F} - I)X(X) + w(X). \tag{1}$$

The Taylor model is contained in the present model by setting $w(X) = 0 \forall X \in \mathscr{B}$. Assuming the displacement fluctuation $w(\partial\mathscr{B})$ to vanish or to be periodic on the boundary of the RVE, the global deformation gradient $\bar{F}$ can be shown to be equal to the mean value of the local deformation gradient F, where the corresponding average is taken over the volume in the initial placement κ_0 (see Ref. [6], p. 363)

$$\bar{F} = \frac{1}{V_0}\int_{\kappa_0(\mathscr{B})} F(X)\,\mathrm{d}V_0 \tag{2}$$

A similar expression can be found for the Cauchy stress. Here the integral has to be taken over the volume in the actual placement κ

$$\bar{T} = \frac{1}{V}\int_{\kappa(\mathscr{B})} T(X)\,\mathrm{d}V. \tag{3}$$

2.2. Boundary conditions

In order to obtain the overall stress response $\bar{T}$, we have to impose displacement boundary conditions on the RVE. There are several approaches to this problem.

2.2.1. Homogeneous boundary conditions

In this case, the displacements on the boundary of the RVE are exactly prescribed by the global uniform deformation $\bar{F}$. This approach is very simple because it uses standard features of most commercial FE codes. Such boundaries, however, are less flexible than the ones that allow fluctuations and, there-

fore, can be expected to result in a spurious global stiffening of the RVE. This effect decays with distance from the boundary and will be less pronounced for RVE shapes with a small ratio of boundary affected volume to total volume. This ratio is most favorable for a spherical RVE shape, and decreases with its diameter. On the other hand, for plate-like RVEs, this effect will be more influential.

2.2.2. Embedding

In this approach the boundary conditions are specified exactly as in the former case. The difference is that the averaging procedure is restricted to an inner region of the structure. The outer region is filled quite arbitrarily either with additional grains or with some more or less equivalent homogeneous material. Since the displacement fluctuations at the boundary of the inner region are in general neither vanishing nor periodic, the averaging formulas, Eqs. (2) and (3), for $\bar{T}$ and $\bar{F}$, respectively, then hold only approximately. This approach is demonstrated in Ref. [8], where the averaging procedure is restricted to 1000 of 4096 elements.

2.2.3. Periodic boundary conditions

Here, the displacement fluctuation field is forced to be periodic by setting it equal at corresponding points of opposite boundaries. Using the displacement split formulation, this can be done independently of the conditions for the overall average deformation. The authors favour periodic boundary conditions because they avoid the stiffening effect of homogeneous boundary conditions without having to calculate a structure outside the RVE as in the embedding approach. Moreover, these conditions are consistent with the philosophy of the RVE concept which describes the structure by a periodic patchwork.

3. Finite element implementation

3.1. Spatial discretization

For the calculation of the stress response to a given deformation process, we use a three-dimensional nonlinear finite-element approach. The RVE is discretized by constant strain tetrahedral elements. A formulation for finite deformations is found in Ref. [7]. The minimal number of elements is determined by the required grain number and deformation resolution inside the grains. Taking one element per grain, we obtain the maximum number of different lattice orientations at the cost of strain field resolution.

The nodal displacement vectors u_K are decomposed according to the global displacement split:

$$u_K = (\bar{F} - I) X_K + w_K \tag{4}$$

with X_K the initial position of node K, and w_K the actual nodal fluctuation. Using this decomposition, the application of homogeneous or periodic boundary conditions follows simply by a reduction of the global system [5].

3.2. Initial grain orientations

As a first example, the initial state for our simulations was chosen to be isotropic. Such isotropy can be expected for polycrystals consisting of a large number of randomly oriented grains. However, the isotropy is very poor for small grain numbers [9]. A considerable improvement can be obtained by an optimization starting from random orientation sets. The orientation space is endowed with a natural metric. Then the distance between all orientations is maximized. This leads to a non-linear optimization problem which can be iteratively solved by standard procedures. The result of such a procedure is a local maximum. In most cases, it is extremely difficult to find and prove global maximality of such a solution, but isotropy tests show us immediately, whether the solution is sufficiently isotropic. In any case, experience shows that RVEs produced in such a way behave sufficiently isotropic even for a rather small number of grains.

4. The constitutive model

Each grain is assumed to be a single crystal. The stresses are determined by the elastic deformations of the lattice, whereas the inelastic deformations relate material vectors to current lattice vectors. The model is based on the assumption of elastic ranges, in which the stresses are determined by a linear, anisotropic law

$$S = \mathbb{K}_t[C - C_{U_t}], \tag{5}$$

$S := F^{-1}TF^{-T}$ being a material stress tensor, C the right Cauchy Green tensor, C_{U_t} that one of an unloaded placement and $\mathbb{K}_t$ the forth order elasticity tensor. The index t indicates the time dependence of this law, which is related to the current elastic range. This time dependence can be removed by the second assumption, which states, that the elastic laws of all possible elastic ranges are isomorphic. As a result, the current elastic law can be transformed into a time-independent reference law by the isomorphy condition

$$\mathbb{K}_t[C - C_{U_t}] = P\mathbb{K}_0[P^T C P - C_{U0}]P^T, \tag{6}$$

where P is an invertible second order tensor, called plastic transformation [4,3].

The linear elastic behaviour of cubic-face-centered single crystals is described by three constants. For the numerical simulation the following parameters have been used: $E = 63$ GPa (Young's modulus), $G = 28$ GPa (shear modulus), $\nu = 0.36$ (Poisson's ratio) [10].

In single crystals quasi-static plastic deformations at room temperature arise almost solely from slip mechanisms on specific crystallographic planes. In the numerical example the slip system theory with octahedral slip systems is applied. As long as the absolute value of the resolved shear stresses

$$\tau_\alpha = \mathrm{tr}(SCd_\alpha \otimes n^\alpha) \tag{7}$$

of all slip systems $\{d_\alpha, n^\alpha\}$ (shear direction, shear plane normal) are below the critical ones $\tau_{c\alpha}$, no slip occurs and P remains constant. If, however, $|\tau_\alpha| \geq \tau_{c\alpha}$, the slip system can be activated and P evolves according to the evolution equation

$$\dot{P}P^{-1} = \sum_\alpha - \dot{\mu}_\alpha d_\alpha \otimes n^\alpha, \tag{8}$$

where the sum is taken over all active slip systems. $\dot{\mu}_\alpha$ is the slip rate in the particular slip system. This rate is assumed to be related to the resolved shear stress by a Bingham-type constitutive relation

$$\dot{\mu}_\alpha = \frac{1}{\eta}\mathrm{sg}(\tau_\alpha)|\tau_\alpha - \tau_{c\alpha}|. \tag{9}$$

As a result, the material is elasto–viscoplastic. By the material formulation, it also holds under finite deformations, as the Euclidean invariance requirements are automatically fulfilled.

The hardening is assumed to be isotropic on the slip system level. The critical shear stress rate is proportional to the shear rate as well as the difference between the present and a saturated critical shear stress. The critical shear stresses are assumed to be initially equal in all slip systems and can be affected by slip in the same slip system (self hardening) and in the other ones (latent hardening). The ratio of latent to self hardening coefficient is assumed to be 1.4. The evolution equation for the critical shear stresses is given by

$$\dot{\tau}_{c\alpha} = h_0 \sum_\beta h_{\alpha\beta} \frac{\tau_{sat} - \tau_{c\beta}}{\tau_{sat} - \tau_{c0}} \dot{\mu}_\beta, \tag{10}$$

$$h_{\alpha\beta} = \begin{cases} 1 & \text{if } \alpha = \beta \\ 1.4 & \text{if } \alpha \neq \beta \end{cases}. \tag{11}$$

The constants $\tau_c = 0.1$ GPa, $h_0 = 0.08$ GPa and $\tau_{sat} = 0.164$ GPa were chosen so that Eq. (10) fits a slip system hardening relationship given by Becker [1]. This relationship was determined on the basis of uniaxial tension tests. The tensile axis of the sheet specimen was perpendicular to the rolling direction. Becker [1] calibrated the hardening response such that the predicted stress–strain-curve determined by a Taylor-like model using 800 crystal orientations matched the test data.

5. Simulated processes

Williams [11] determined the texture, produced by simple shear in a polycrystalline sample of aluminium. For his study, he used commercial cold-rolled aluminium. The aluminium sample has been sheared perpendicular to the rolling-direction up to a shear magnitude k of 2.2. For a spherical X-ray sample cut out of the specimen, Williams obtained (111) and (100) pole plane projections in the plane containing the shear direction and the shear plane normal.

In the numerical simulation of the shearing process, an RVE with $7 \times 7 \times 7$ nodes is used. The

structure contains 1080 tetrahedral elements and 645 degrees of freedom. Combining five tetrahedral elements in one grain, there are initially 216 independent orientations in the RVE. Due to the inhomogeneity of the deformation process, the orientations within the grains become inhomogeneous.

Starting from the isotropic and stress-free state, a constant, isochoric deformation rate is imposed on the RVE until the global shear number reaches its final value. The strain rate is chosen such that the global stress–strain curve is nearly independent of the viscosity used in the flow rule on the slip system level. The resulting texture is given by the 1080 crystal orientations after a simulated unloading process. The stiffness tensors of the global elastic behaviour are calculated before and after Restraining. Using different yield criteria, initial and subsequent yield surfaces are determined.

6. Results

6.1. Texture

Using linear density distributions assigned to the element orientations, density plots have been constructed (Figs. 1 and 2). The simulations start from a nearly isotropic state, whereas the experiments in Ref. [11] were done with cold rolled sheet material with a corresponding texture. Nevertheless, the location and value of highest density values in the (111) pole figures are in good agreement. However, in the (100) pole figure, two experimental maxima are missing.

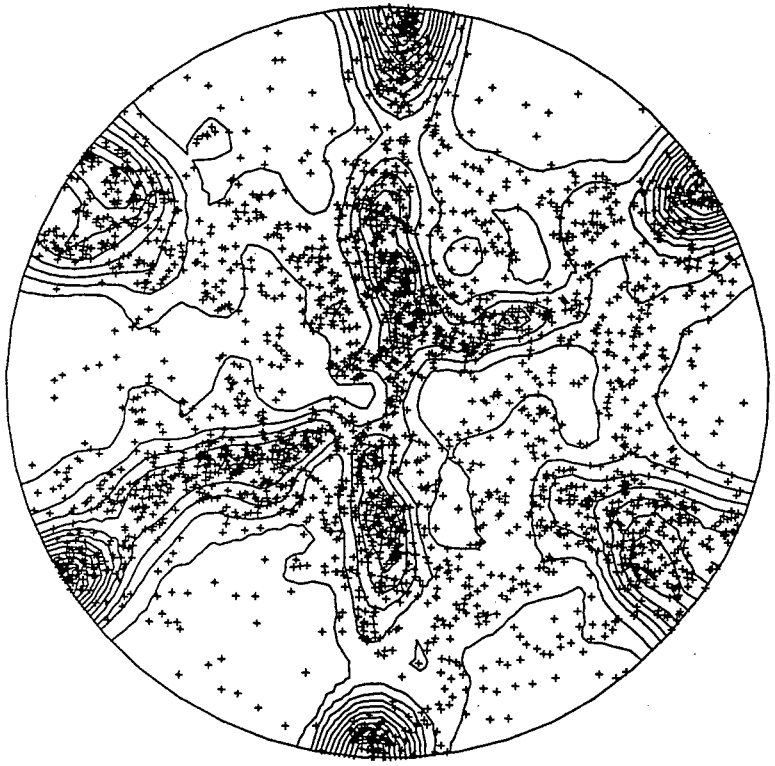

Fig. 1. (111) pole figure of the texture after shearing to $k = 2.2$.

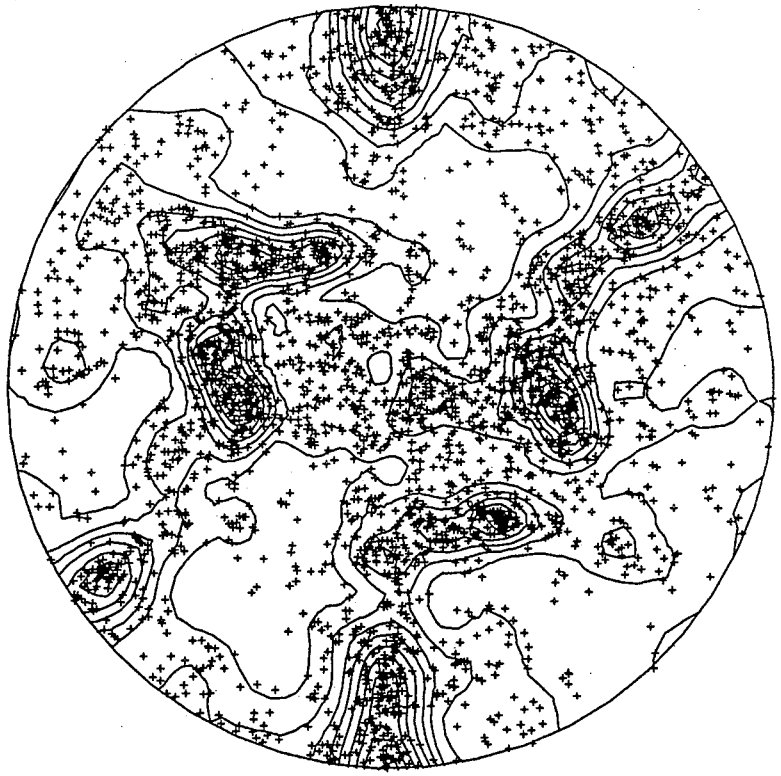

Fig. 2. (100) pole figure of the texture after shearing to $k = 2.2$.

Data from experimentally-determined textures is normally given in the form of two-dimensional pole figures. Simulations, however, provide full three-dimensional information on the individual grain orientations. An appropriate representation of these results is the Rodrigues space is used, for example, in Refs. [1,2]. Choosing a fixed reference orientation, any given orientation can be represented by a spatial rotation with respect to the reference one. This rotation has an axis $\boldsymbol{n}$ and an angle φ between 0 and 180°. As such, the Rodrigues vector is a vector $\boldsymbol{r}$ of direction $\boldsymbol{n}$ and length $|\boldsymbol{r}| = \tan(\varphi/2)$.

In the inverse pole figure, reduction using fcc crystal symmetries leads to the orientation triangle. A similar reduction can be performed in Rodrigues space. The fundamental region has the shape of a cube with the corners cut off, centered at 0.

Using density distributions as for the pole figures, a continuous density field in the Rodrigues space is obtained. It is visualized as 3D plots or as set of 2D sections. The latter approach is frequently found in the literature on 3D texture analysis.

Fig. 3 contains density plots in 21 equidistant sections covering the fundamental region (coordi-

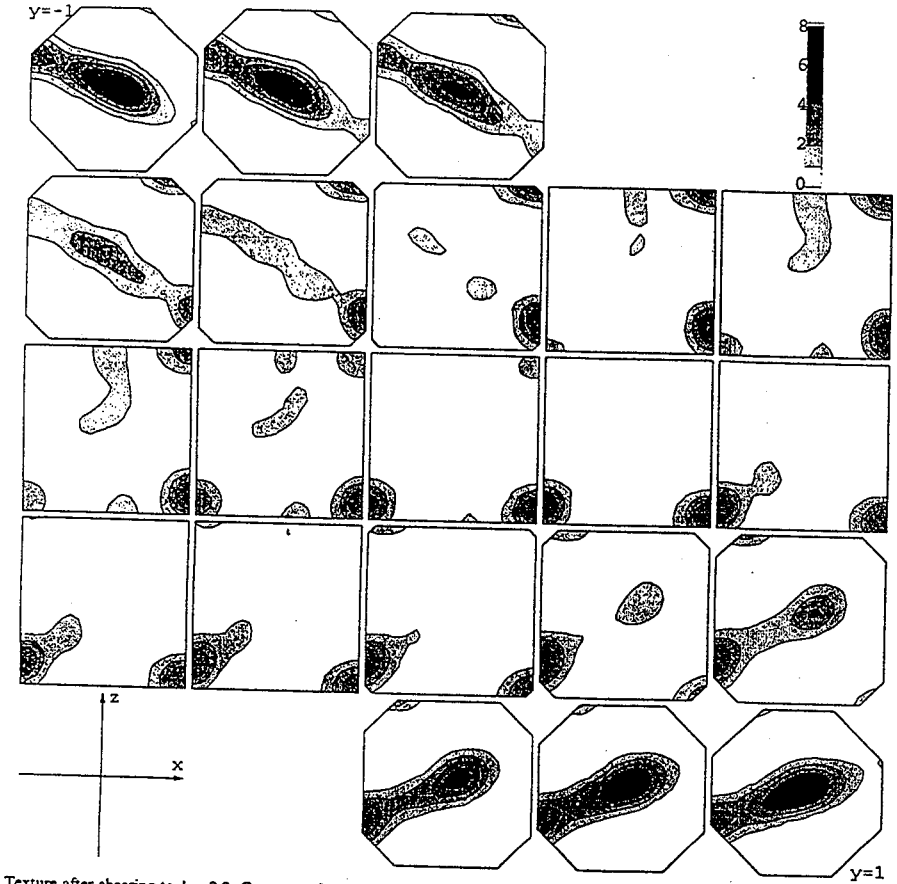

Fig. 3. Texture after shearing to $k = 2.2$. Contours of normalized orientation density in equidistant sections in the fundamental region of the Rodrigues space for cubic symmetry. Sections are parallel to the shear plane, x is the shear direction.

nates in Rodrigues space normalized according to Ref. [2]). The regions of increased density are located near the boundary. Considering the relations between opposite faces of that region, the orientations are found to cluster in a continuous band, which stands for an incomplete [110] fiber in the shear direction and a partial (111) fiber corresponding to the shear plane. The highest density values are observed at the stable (101)[010] orientation ($x = 0$, $y = \pm 1$, $z = 0$) [4].

6.2. Elastic behaviour

By imposing six linear independent elastic deformations on the RVE, the global stiffness tensor is calculated. It turns out that the elasticities remain almost isotropic during deformation. Because of the weak anisotropy of the single crystalline aluminium and the spatial distribution of the crystal orientations, the anisotropy of the aggregate is negligible. In the initial and the distorted state, the Lame constants are given by $\lambda = 57.67$ GPa and $\mu = 26.02$ GPa.

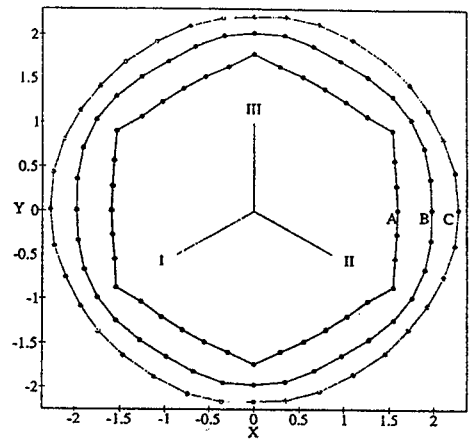

Fig. 4. Initial yield surfaces for different values of the power criterion ($A = 3\%$, $B = 50\%$, $C = 99\%$), p.

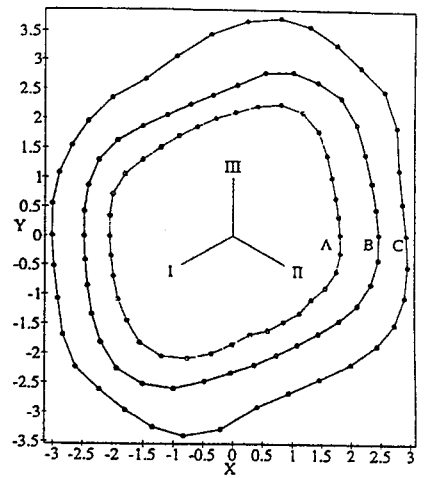

Fig. 6. Yield loci at $k = 2.2$, (power crit. $A = 40\%$, $B = 70\%$, $C = 95\%$.)

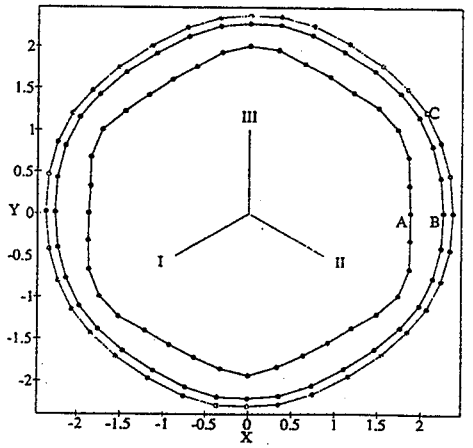

Fig. 5. Initial yield surfaces for different values of the residual strain criterion d ($A = 0.01\%$, $B = 0.1\%$, $C = 0.2\%$).

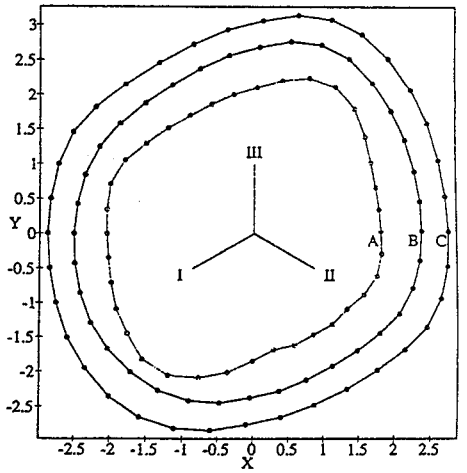

Fig. 7. Yield loci at $k = 2.2$, (strain crit. $A = 0.01\%$, $B = 0.1\%$, $C = 0.2\%$.)

6.3. Inelastic behaviour

To determine the initial yield surface, isochoric deformation processes have been performed such that the stress paths in the Haigh–Westergaard-stress-space are equidistant. On these stress paths, different yield criteria are evaluated. In experiment, the yielding of a specimen can be indicated by different measures. Common examples are the residual deformation after an elastic unloading process, or the deviation of the stiffness from the pure elastic value. The RVE model offers the facility to use the physically relevant information about the slip system activity. The ratio of the mean dissipation rate p_{diss} to the total stress power p_{tot} defines a normalized average indicator for yielding

$$p = p_{\text{diss}}/p_{\text{tot}}, \quad p_{\text{diss}} = \frac{1}{V_t}\int_{V_t}\sum_{i=1}^{12}\tau_i\dot{\mu}_i\,\mathrm{d}V, \quad p_{\text{tot}} = \operatorname{tr}(\tilde{T}\tilde{D}) \tag{12}$$

with the macroscopic strain rate $\tilde{D}$. As the global stress–strain-curve is nearly rate independent, the residual strain after an elastic unloading can be estimated by the present stress and the known elastic law. A one-dimensional measure d can be defined as the Frobenius norm of the residual strain.

Figs. 4 and 5 show the indicators in the Haigh–Westergaard-stress-space. The projection of the axes of the main stresses in this space are symmetry lines of the yield loci. On the basis of these results, the aggregate can considered to be isotropic with respect to the transition from elastic to inelastic behaviour. Furthermore, it turns out that fine criteria ($p \approx 3\%$, $d \approx 0.01\%$) are of Tresca type, coarse ones ($p \approx 50\%$, $d \approx 0.1\%$) tend to the v. Mises type.

Figs. 6 and 7 show the yield loci of the sheared RVE. Due to the accumulation of residual stresses the power criterion does not start at $p = 0$ in the globally unloaded state. The transition behaviour is anisotropic due to texture development and accumulated residual stresses.

7. Conclusions

Using a model for the description of finite inelastic deformations of single crystals, as well as the concept of a representative volume element, simulations of shear tests on polycrystalline specimens as reported in Ref. [11] have been carried out. Due to lack of data, assumptions concerning the initial texture had to be made. In order to identify particular aspects of the texture development, a representation in Rodrigues space was used.

In addition to the texture features, the initial and subsequent yield loci have been examined using different yield indicators. In the initial state, fine criteria are of Tresca type and coarse ones are of v. Mises type, thus indicating isotropy of the elastic–plastic transition behaviour. As to be expected, this isotropy is completely lost after large plastic deformation.

Based on the displacement split formulation, periodic boundary conditions have been applied to the FE-model by global system reduction.

References

[1] R. Becker, Analysis of texture evolution in channel die compression. I. Effects of grain interaction, Acta Metall. Mater. 39 (6) (1991) 1211–1230.
[2] R.C. Becker, S. Panchanadeeswaran, Crystal rotations represented as Rodrigues vectors, Textures Microstruct. 10 (1989) 167–194.
[3] A. Bertram, M. Kraska, Description of finite plastic deformations in single crystals by material isomorphisms, in: D.F. Parker, A.H. England (Eds.), IUTAM Symposium on Anisotropy, Inhomogeneity and Nonlinearity in Solid Mechanics, Kluwer Academic Publishers, Nottingham, UK, 1994, pp. 77–90.
[4] A. Bertram, M. Kraska, Determination of finite plastic deformations in single crystals, Arch. Mech. 47 (2) (1995) 203–222.
[5] M. Kraska, A. Bertram, Simulation of polycrystals using an FEM-based representative volume element, Techn. Mech. 16 (1) (1996) 51–62.
[6] A. Krawietz, Materialtheorie, Springer, 1986.
[7] J.T. Oden, Finite Elements of Nonlinear Continua, McGraw-Hill, 1972.
[8] G.B. Sarma, P.R. Dawson, Effects of interactions among crystals on the inhomogeneous deformations of polycrystals, Acta Mater. 44 (1996) 1937–1953.

[9] H. Takahashi et al., Elastic–plastic finite element polycrystal model, Int. J. Plast. 10 (1) (1994) 63–80.
[10] Ch. Weißmantel, C. Hamann, et al., Grundlagen der Festkörperphysik, Deutscher Verlag der Wissenschaften, Berlin, 1979.
[11] O.W. Williams, Shear textures in copper, brass, aluminum, iron and zirconium, Trans. Met. Soc. AIME 224 (1962) 129–139.